Laboratory Study of the Active Debris Removal Algorithms on Air-Bearing Test Bed

Akhloumadi Mahdi[1], Kozin Filipp[2], Danil Ivanov[2]

[1]Moscow Institute of Physics and Technology (State University), Institutsky lane, Dolgoprudny, Moscow Region, Russia
[2]Keldysh Institute of Applied Mathematics RAS, Miusskaya sq. 4, Moscow, Russia

akhloumadi@gmail.com

Abstract. Space debris removal is one of the most important problems in space exploration. This work is devoted to the development and testing of control algorithms for microsatellites mock-ups on an aerodynamic table. The mock-ups are equipped with thrusters simulators to control the motion of the center of mass and angular motion on the plane of the table. The aim of the work is to construct a control algorithm using virtual potential functions and apply it to the problems of rendezvous and docking. Simultaneously with these tasks, the problem of avoiding a collision with an object in the event of a dangerous approach not from the docking side is solved. Also the algorithm for autonomous debris observation of the 3U CubeSat is proposed. The results of the control algorithm tests are presented in the paper.

1. Introduction

Currently, there are different approaches to solving the problem of space debris. One of the ways is to launch special small spacecraft that are able to attach to a non-cooperative object and, using a propulsion system, change the orbit of space debris. With such a debris removal scheme, the task of controlling the relative motion of the spacecraft during the approach to an arbitrarily rotating object arises. To increase the probability of mission success, the developed control algorithms are tested in ground conditions using special laboratory stands. The rendezvous and docking control algorithms are commonly verified on the test-bed allowing frictionless motion along the surface of a smooth table. The air cushion between the mock-up legs and the surface is used in most cases. It is often produced by the on-board stowed compressed air. This greatly limits the duration of the experiments. Overview of such facilities is presented in the survey paper [1]. Another way to produce the air cushion is to create the airflow through the grid of holes in the flat table surface (air-hockey table). The air-injection system connected to the reservoir under the table surface is necessary. Such a facility is installed at the Keldysh Institute of Applied Mathematics [2–4].

The active space debris removal using small satellite can be divided at several stages. First, the space debris should be observed from safe relative distance in order to determine its angular motion and possible point for the capturing. For this stage the natural closed relative trajectory should be obtained by the active satellite control system. However, due to disturbances the relative drift can appear. In that case if the relative distance between the satellite and the debris become dangerous a collision avoidance maneuver should be applied, moreover after its execution the relative distance should remain suitable for the debris observation. After the capturing point is determined, the stage of

the rendezvous and capturing maneuver follows. At this stage the most crucial is also preventing the collision in the case of approaching of the debris not from the point of capturing. In this paper the algorithms for this two stages are proposed and tested on the aerodynamic test bed.

1. Laboratory facility description

Laboratory facility COSMOS (COmplex for Satellites MOtion Simulation) consists of the microsatellites mock-ups (Figure 1) placed on the air-bearing table, industrial fan and its control unit, and air supply system (Figure 2). The air bearing table includes the flat perforated aluminum surface and special cavity underneath where the air builds up. The surface of the table consists of two one-cm thick plates. The plates are fixed by a special frame that prevents bending due to the weight of the plates and excessive pressure. The resulting surface unevenness is about 3.5 mm. The total surface area is 198 by 148 cm. The surface has the pattern of 1 mm diameter holes with 20 mm intervals. The distance between the holes is chosen to provide almost frictionless motion for 30 cm diameter mock-up of up to 6 kg mass. The mock-ups have the shape of an octagonal prism of 40 cm height. Each side has mounting holes that allow hardware installation both inside and outside.

The mock-ups are based on the Orbicraft and Orbicraft-pro construction kit developed by SputniX Ltd [5]. The mass of the bigger mock-up is about 5.2 kg, the axial moment of inertia is about 0.05 $kg \cdot m^2$, the mass of the CubeSat-based is about 1.1 kg, the axial moment of inertia is about 0.01 $kg \cdot m^2$. Control system imitator includes:

- on-board computer Raspberry PI 2 B;
- power supply system (battery and power management unit);
- set of sensors: magnetometer, Sun sensors, angular velocity sensor, accelerometer;
- set of actuators: reaction wheel, four propellers for the thruster imitation;
- data exchange system;
- on-board camera;
- Wi-Fi module.

There is a special mark on top of each mock-up. The position and attitude of the mock-up is determined using external video camera data processing [6]. This information is transmitted via Wi-Fi channel to the on-board computer. It is then used to generate a control command. In case of autonomous attitude and position determination, the video camera is used as an independent external motion determination system.

The test-bench disturbances were estimated experimentally. Preliminary experiments showed that the air flow from the holes is stationary, i.e. does not vary with time, but rather depends on the location on the table surface. Disturbances acting at some point of the table are almost stationary. So a map of forces and torques acting on the mock-up on the surface of the table may be constructed. This map was constructed by processing the information of the free motion of the mock-up. External video state determination system was used. Linear and angular accelerations of the mock-up were estimated.
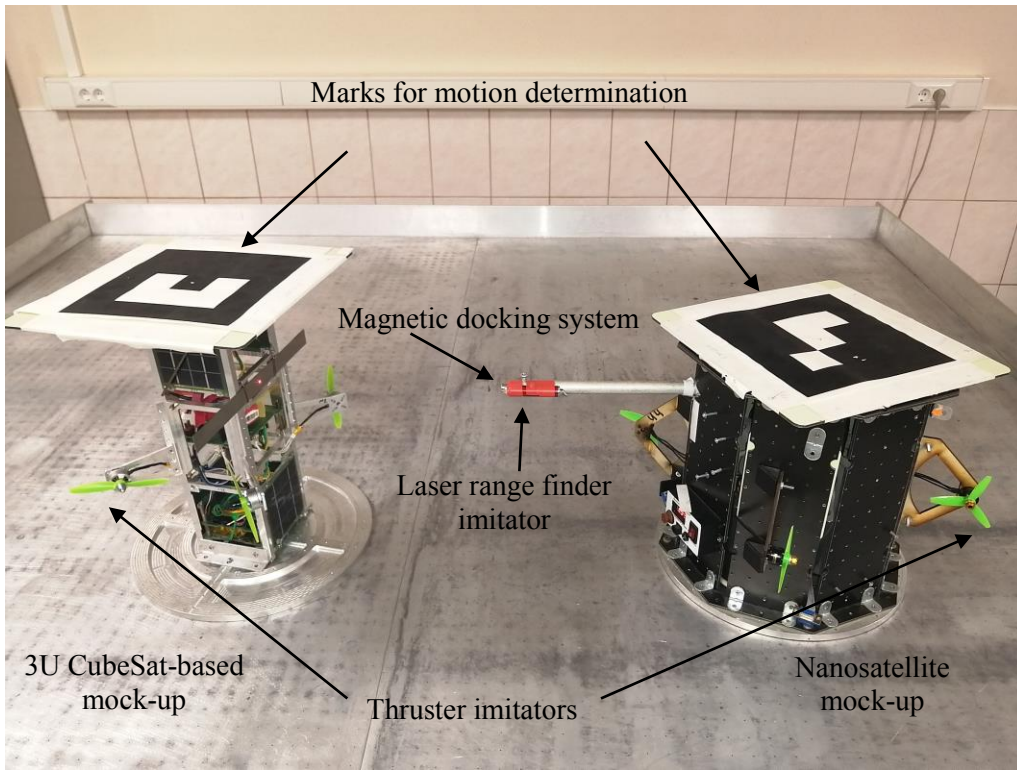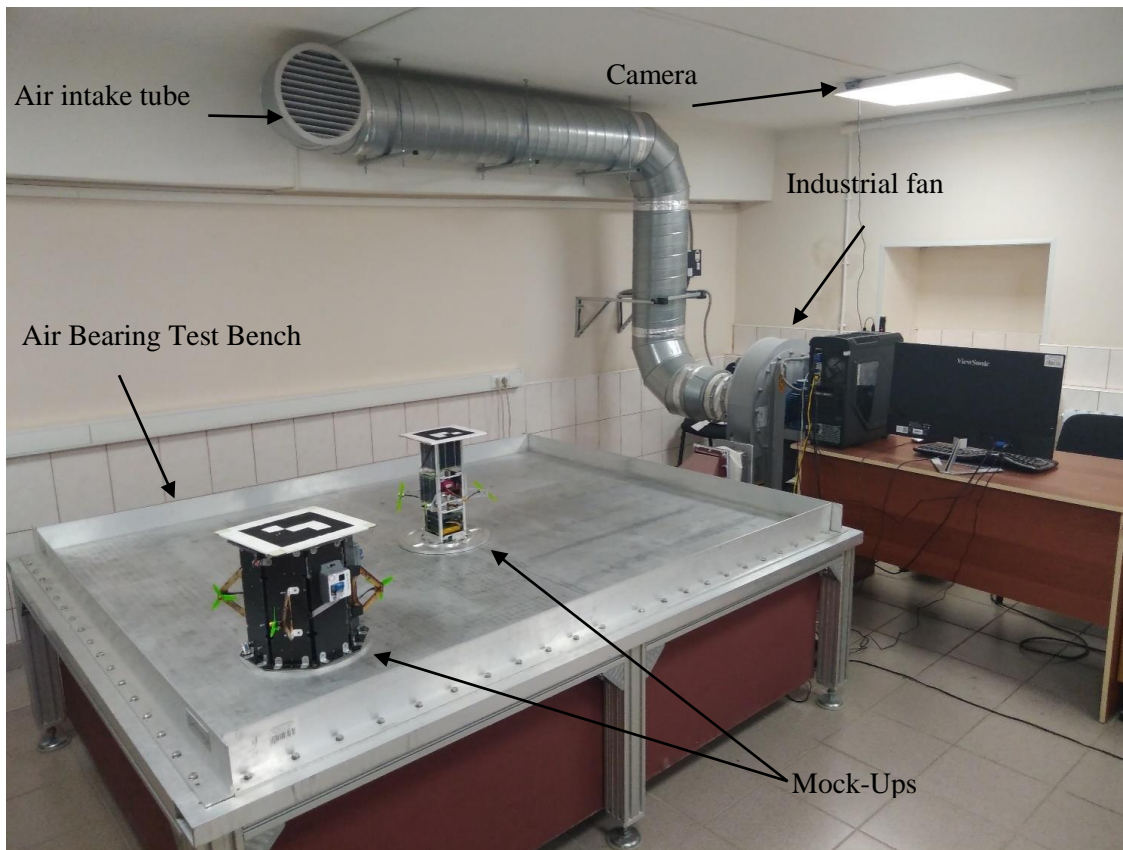
F**igure. 1.** Nanosatellite mock-ups

Figure. 2. Test facility COSMOS at the Keldysh Institute of Applied Mathematics

2. Controlled motion for debris observation

Consider the space debris and active satellite on the near circular orbits. For a long observation it is reasonable to choose a natural closed relative orbit. Such an orbit can be obtained using Clohessy-Wiltshire equations which has the following form:

$$\ddot{x} = -2\dot{z}\omega,$$
$$\ddot{y} = -y\omega^2,$$
$$\ddot{z} = 2\dot{x}\omega + 3z\omega^2$$

(1)

where $\mathbf{r} = \mathbf{r}_2 - \mathbf{r}_1 = (x, y, z)$ is the relative state vector in the orbital reference frame moving in the circular orbit with orbital angular velocity ω. The solution of (1) is

$$x(t) = -3C_1\omega t + 2C_2 \cos \omega t - 2C_3 \sin \omega t + C_4,$$
$$y(t) = C_5 \sin \omega t + C_6 \cos \omega t,$$
$$z(t) = 2C_1 + C_2 \sin \omega t + C_3 \cos \omega t$$

(2)

where the constants $C_1, C_2, C_3, C_4, C_5, C_6$ are defined by the initial conditions. In the common case the trajectory is elliptical spiral. The term responsible for the relative drift is $-3C_1 \omega t$. The relative trajectory of two satellites is closed if and only if $C_1 = 0$. However, ideal initial conditions for a closed free motion cannot be achieved and it lead to slow change of instant ellipse position. To stop the drift the following Lyapunov-based control along the x-axis can be applied:

$$u_x = -kC_1, \ k > 0$$

(3)

Consider the case when the active satellite observe the debris staying at the negative part of the x-axis. Assume that the observing sensors requires the maximal distance of R_{max}. So, this value should not be achieved by the instant position of the ellipse in the case of zero drift is $C_4 - a$, where $a = \sqrt{C_2 + C_3}$ is the major semi axis of the ellipse and C_4 is instant position of the center of the ellipse along x-axis. Form the other hand in the observing stage the dangerous distance is also can be set as R_{min}, where the collision with debris is possible. The closest distance can be calculated as $C_4 + a$. To avoid the collision the bang-bang control can be applied. For the impulsive thrust the algorithm can be described as follows:

$$u_x = \begin{cases} -2\omega C_1 / dt, \ if \ |C_4 + a| < R_{min} \\ -\omega C_1 / dt, \ if \ |C_4 - a| > R_{safe} \end{cases}$$

(4)

When the dangerous distance is reached, the control changes the sign of the relative drift constant C_1 and the relative distance is increasing. When the distance reaches a safe distance R_{safe} that is less than R_{max} the drift is stopped by the second impulse. The similar approach can be applied if the satellite distance is approaches the maximal value R_{max} that is not suitable for the debris observation.

Such a control scheme is quite simple but it is reliable and robust. The most crucial problem in the observing stage if the relative motion determination. Assume that the active satellite equipped with laser range finder and the optical sensor for the pointing. The measurements of the laser range finder provide the distance to the debris and the optical sensors measures the unit vector direction angles in the orbital reference frame. This measurements are processed by the Kalman filter algorithm which estimate the 6-th dimensional state vector – relative position vector and relative velocity. Using this estimations the semi axis a and relative shift C_4 can be calculated. Since the optical sensors cannor

measure in the shadow part of the orbit the current state vector is obtained by the integration of the motion equations using last obtained state vector. Since it is calculated with errors the covariance matrix can be used to calculate the error ellipse of the current and expected state vector.

Such a scheme of the motion of the active satellite for debris observation is implemented numerically. Figure 3 shows the relative trajectory of the active satellite, debris, dangerous distance and error ellipsoid. The relative position errors can be seen from Figure 4. The increase of the error is caused by absence of the measurements in the shadow part of the orbit. The relative distance is demonstrated at Figure 5. Initially the relative drift result in decreasing the distance but at the dangerous distance the impulse was applied and the satellite started drifting with another sign. When the safe distance was achieved the second impulse stopped the drift and the ellipse become almost closed.
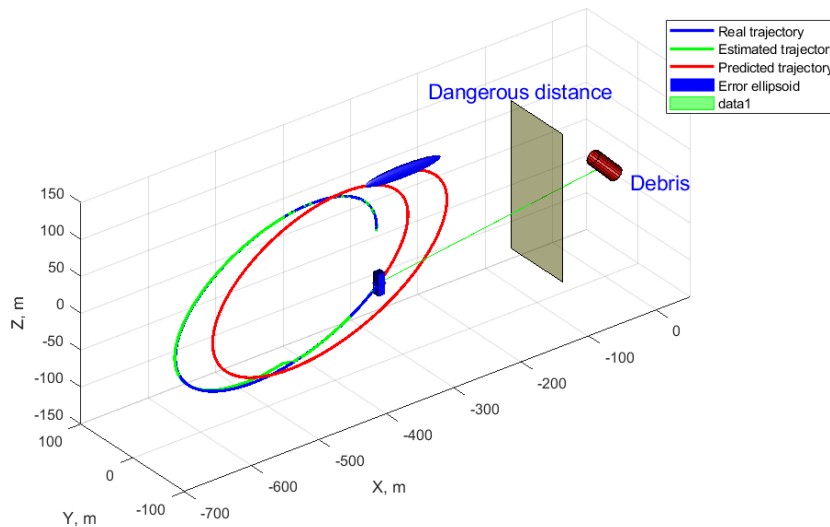

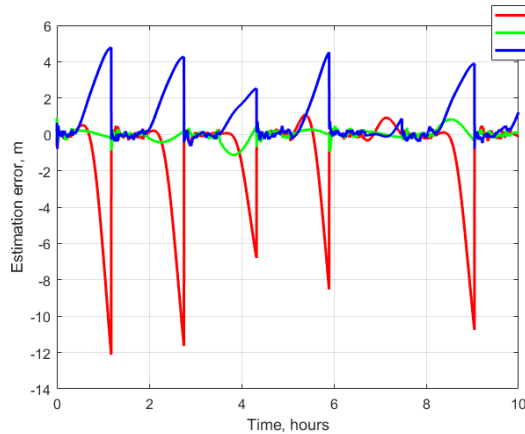**Figure. 3.** Relative trajectory of the active satellite at the debris observation stage

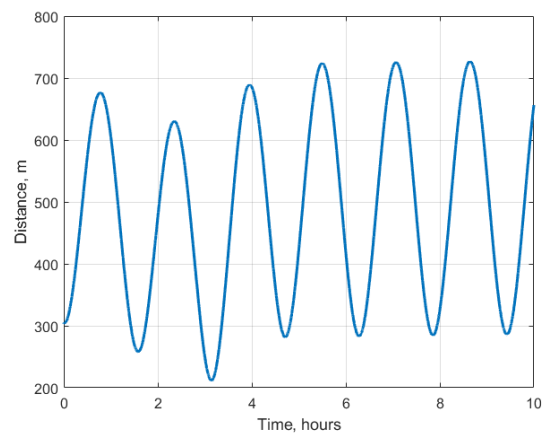| **Figure 4.** Relative position estimation errors	**Figure 5.** Relative distance

The proposed scheme was tested using laboratory facility. One of the mock-ups is fixed on the table, the other is imitating active satellite. The orbital free motion is considered only in the orbital plane since the out-of-plane motion is always bounded that is suitable for the observation. The free orbital motion trajectory is calculated according to the orbital initial conditions and tracked by the on-board control system. Figure 6 shows the relative trajectory of the active mock-up relative to the debris mock-up. Initially trajectory has a drift towards the debris mock-up. At the dangerous distance of 0.4 m the collision avoidance manoeuvre was applied that changed the drift sign and the distance

increased after two revolutions. After reaching the safe distance of 1m the drift was stopped by the second impulse as one can see on Figure 7. During the relative motion the laser range-finder imitator was pointed towards the debris. Figure 8 shows the required pointing angle and implemented by the control system. Its difference does not exceed 3-4 deg.
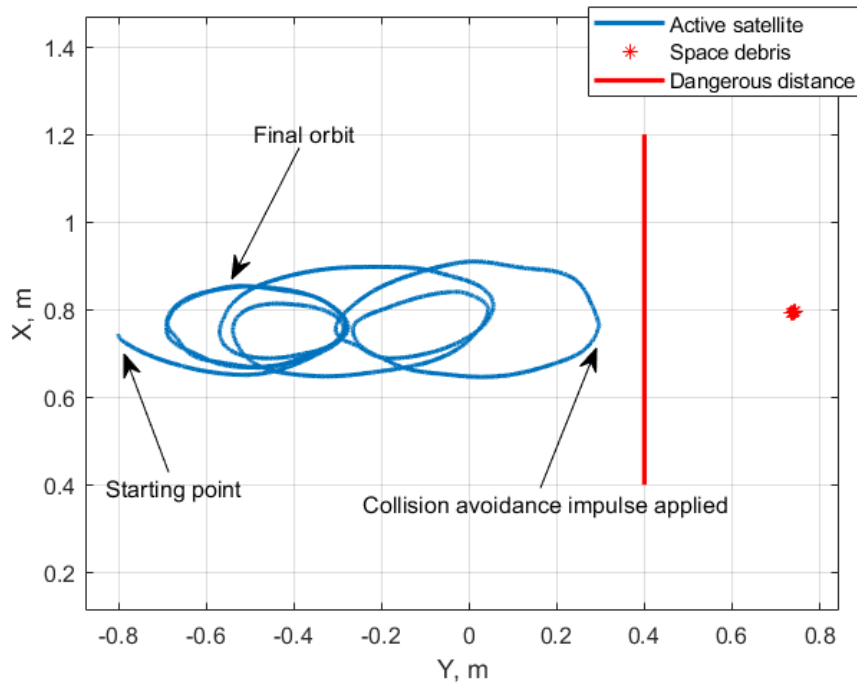

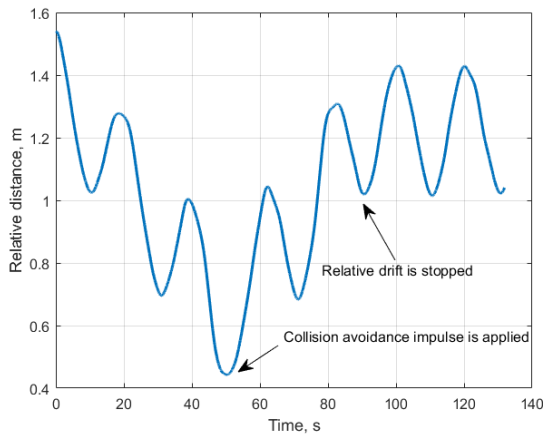**Figure 6.** Trajectory of nanosatellite mock-up on air table
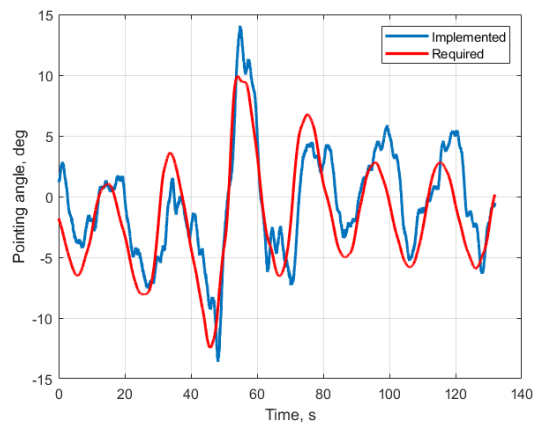

Figure 7. Relative distance

Figure 8. Pointing angle: required and implemented

Thus, the simple relative motion control for debris observation is proposed and successfully tested on the air-bearing table. The orbital motion is imitated on the table only partly and the achieved accuracies will be not the same for the intended mission, nevertheless it demonstrates the controlled motion scheme implemented in hardware.

3. Capturing maneuver using potential-based control

The uncooperating tumbling target representing space debris on air bearing table has to be captured as the final goal of mission. The nanosatellite mock-up, which is equipped with propellers, has to accomplish this task.

The dynamic of mockups can be modeled as parallel-plane motion as there are only 3 degrees of freedom. The attitude of rigid mockup is expressed by an angle θ in its body reference frame and its position by x, y in inertial reference frame as seen in Figure 5. Figure shows the attitude and position of mockup with respect to the target. First task is to avoid collision with obstacles in way to the target. The second task is to align the attitude direction vector of mockup as $\overrightarrow{SN}$ with its counter vector $\overrightarrow{TN}$ of target. In addition to this condition, the points E on both objects most coincide with each other with zero speed. The docking can be modeled with these two later conditions. To meet the requirements the proper control algorithm for both phases of approaching and docking has to be designed. The whole scenario can be expressed as follow: the mockup directly approaches to the target while keep a safe distance from obstacles appearing in way. Keeping its capturing point toward the center of mass of the target. When it arrives to a close distance of target it waits for the docking window of the rotational target to be opened. When the window shows up the mockups implements the docking. The third important task is to determine the acceptable values of the parameters of the attractive/repulsive potential function control algorithm. This task will be accomplished in an analytical way by using Lyapunov methods and Routh–Hurwitz stability criterion.

For the approaching phase in the center of mass off the target, a potential function is set. The obstacles are the poles of some repulsive potential functions. In the docking phase the another attractive potential function is produced with respect to the rotational speed of the target.
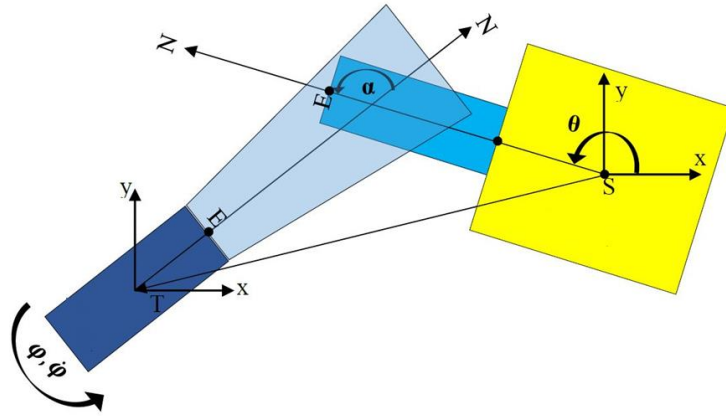

Figure 9. Relative position and attitude of mockup and the target

The equation of potential function can be chosen as follow:

$$V = -c_a e^{\frac{-z}{l_a}} + c_r e^{\frac{-z}{l_r}} \tag{5}$$

In (5) the C_a, C_r, l_a, l_r are the geometrically coefficients of the potential function. z is the distance from the pole. In (5) First part is the attractive source and the second is the repulsive. the pair of C_a, C_r representing the strength of the potential field and the l_a, l_r are the corresponding lengths. For obstacles $C_a = 0$ and for the target in approaching phase both C_a, C_r are some real positive numbers. In docking phase $C_a \neq 0$ amplified due to the time of docking. As the key definition of potential

function, any force can be the gradient of a potential function. The control force **F** can be represented as derivative of a potential function:

$$-\nabla V = \mathbf{F} \tag{6}$$

Using the stability analysis it is possible to choose such a parameters of the potentials to provide asymptotical stability of the predefined relative distance between the two mock-ups.

The capturing scenario is shown in Figure 10. The chaser waits in a safe desirable distance for the window with required attitude for the capturing to be opened and then it docks to it. It is realized by selective repulsive second term in (5) that is set to zero in the suitable for capturing angles. The required attitude is achieved using PD regulator.
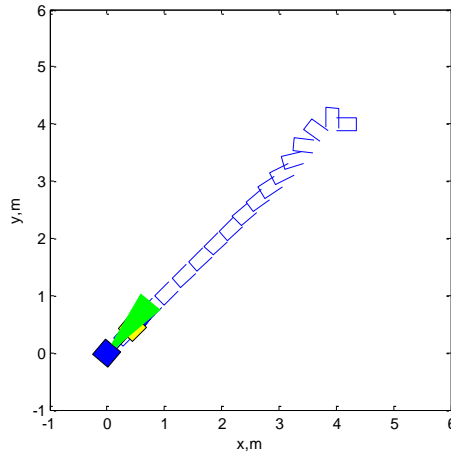

Figure 10. Motion during capturing phase

This capturing algorithm were tested on the air bearing table for simulating the rendezvous and docking. Initially both mock-ups where located at different parts of the air bearing table. The target mock-up is passively mowing along the table imitating non-cooperative space debris. The active mock-up starts to move towards the debris but it can dock to it only in predefined sector, where the magnetic capture is possible. So, in case the relative orientation is not appropriate the active mock-up stands in the equilibrium position of about 0.8 m. All the control is calculated using artificial potential functions with precalculated parameters $C_a = 30, C_r = 5, l_a = 3, l_r = 0.2$.

Figure 11 shows an example of relative distance during one of the experiment with docking algorithm. The relative velocity is presented in Figure 12. First several seconds the active mock-up moves towards the target, but the attitude was inappropriate for capturing, so the collision avoidance potential keep the mock-up at the equilibrium distance. During the next 30 seconds the arbitrary relative attitude motion of the mock-ups was not appropriate for magnetic docking. And at 28 s after the experiment beginning the final stage of the control was executed. The red star at the Figure 11 and 12 is the point of the successful docking – the relative distance between the mock-ups in the final docked position is 0.4 m.
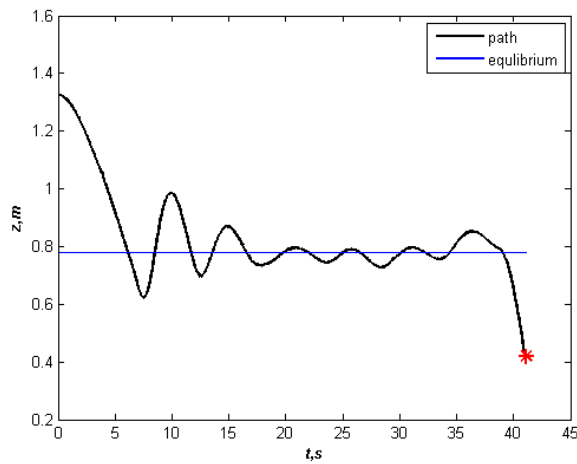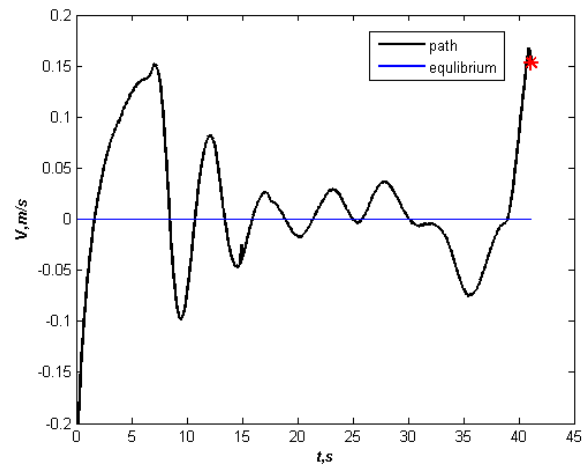
Figure 11. Relative distance during the experiment

Figure 12. Relative velocity during the experiment

4. Conclusions

The proposed algorithms for controlled motion for space debris observation and for capturing using artificial potentials are successfully tested using laboratory facility on the air-bearing test-bed. The scheme of the collision avoidance at the stage of debris observation is simple and easy for implementation. The most critical part for implementation of this relative motion scheme is relative state vector estimation. The proposed algorithm based on extended Kalman filter provides an estimation using laser range finder measurements. Its errors are taken into account in relative distance calculation. At the capturing stage the artificial-potential based control with selective term is proved to be convenient approach in the case of chaotically tumbling space debris. However, the parameters of the control algorithm should be carefully precalculated to provide the required safe distance at the station keeping stage before the capturing.

References
[1]   Rybus T and Seweryn K 2016 Planar air-bearing microgravity simulators: Review of applications, existing solutions and design parameters *Acta Astronautica* **120** 239–59
[2]   Ivanov D S, Koptev M D, Mashtakov Y V, Ovchinnikov M Y, Proshunin N N, Tkachev S S, Fedoseev A I and Shachkov M O 2018 Laboratory Facility For Microsatellite Mock-Ups Motion Simulation *Journal of Computer and Systems Sciences International* **57** 115–30
[3]   Ivanov D, Koptev M, Mashtakov Y, Ovchinnikov M, Proshunin N, Tkachev S, Fedoseev A and Shachkov M 2018 Determination of disturbances acting on small satellite mock-up on air bearing table *Acta Astronautica* **142** 265–76
[4]   Ivanov D, Koptev M, Ovchinnikov M, Tkachev S, Proshunin N and Shachkov M 2018 Flexible microsatellite mock-up docking with non-cooperative target on planar air bearing test bed *Acta Astronautica* **153** 357–66
[5]   "SputniX - Orbicraft" Available: http://sputnix.ru/ru/products/eduru/orbikraft-1-0.
[6]   Koptev M, Proshunin N and Ivanov D 2015 Motion Determination of Microsatellite Control System Mock-Ups on Aerody-namic Testbed Using Monocular Vision *Preprint of KIAM RAS* 32